

1
2
3
4
5
6
7
8
9
10
11
12
13
14
15
16
17
18
19
20
21
22
23
24
25

GPR120 controls neonatal brown adipose tissue thermogenic induction

Tania Quesada-López^{1,2}, Aleix Gavaldà-Navarro^{1,2}, Samantha Morón-Ros^{1,2}, Laura Campderrós^{1,2}, Roser Iglesias^{1,2}, Marta Giralt^{1,2}, Francesc Villarroya^{1,2}.

¹ Department of Biochemistry and Molecular Biomedicine and Institut de Biomedicina (IBUB), University of Barcelona, Barcelona, Catalonia, Spain.

² CIBER Fisiopatología de la Obesidad y Nutrición, Spain.

Correspondence:

Dr Francesc Villarroya

Department of Biochemistry and Molecular Biomedicine

Faculty of Biology, University of Barcelona, Barcelona, Catalonia, Spain.

Avda Diagonal 643

0028 Barcelona. Spain.

Tel. 34 934021525

E mail. fvillarroya@ub.edu

26 **Abstract**

27 Adaptive induction of thermogenesis in brown adipose tissue (BAT) is essential for the
28 survival of mammals after birth. We herein show that G-coupled receptor protein-120
29 (GPR120) expression is dramatically induced after birth in mouse BAT. GPR120
30 expression in neonatal BAT is the highest among GPR120-expressing tissues in mouse
31 at any developmental stage tested. The induction of GPR120 in neonatal BAT is caused
32 by the postnatal thermal stress rather than by the initiation of suckling. GPR120-null
33 neonates were found to be relatively intolerant to cold: close to one-third did not
34 survive at 21°C, but all such pups survived at 25°C. Heat production in BAT was
35 significantly impaired in GPR120-null pups. Deficiency in GPR120 did not modify brown
36 adipocyte morphology or the anatomical architecture of BAT, as assessed by electron
37 microscopy, but instead impaired the expression of UCP1 and the fatty acid oxidation
38 capacity of neonatal BAT. Moreover, GPR120 deficiency impaired FGF21 gene
39 expression in BAT and reduced plasma FGF21 levels. These results indicate that
40 GPR120 is essential for neonatal adaptive thermogenesis.

41

42

43

INTRODUCTION

44

In mammals, the developing fetus does not perform adaptive heat production for the maintenance of body temperature; instead, the body temperature is maintained via maternal thermal homeostasis (10, 19). In most mammalian species, brown adipose tissue (BAT), which is the main site of non-shivering thermogenesis, begins to develop in the late fetal period due to ontogeny-programmed mechanisms, in the absence of environmental thermal stress stimuli (4,17,27). At birth, neonates must rapidly adapt from the warm intra-uterine environment (close to 37°C) to a colder extra-uterine environment. The achievement of this adaptation is crucial, since newborn hypothermia can be lethal (1, 4). Postnatal temperature maintenance is mainly achieved by BAT-mediated non-shivering thermogenesis (1, 4). The post-birth activation of BAT involves the up-regulation of uncoupling protein-1 (UCP1, which is key to providing the mitochondria of BAT with thermogenic properties) and induction of its proton conductance (21), the progressive biogenesis of mitochondria within BAT, and adaptations for active metabolic fuel oxidation to sustain thermogenesis (4,8). Sympathetic activation is believed to induce neonatal BAT thermogenesis in a manner similar to the cold-induced activation of BAT in adults. However, additional factors appear to be involved in the neonatal induction of BAT thermogenesis. For example, high levels of fibroblast growth factor 21 (FGF21) in neonatal plasma, originating in the liver in response to the initiation of milk intake, have been shown to activate neonatal BAT thermogenesis (12). FGF21 favors BAT activation and promotes the browning of white adipose tissue in adults (6, 12). FGF21 is expressed and secreted by the liver, and may also be produced by BAT under conditions that trigger thermogenic activation (13), but the role of locally synthesized FGF21 in neonatal BAT thermogenesis is unknown.

68

We recently identified an additional pathway through which BAT and WAT undergo thermogenic regulation via activation of G-protein coupled receptor 120 (GPR120, also called fatty acid receptor-4, FFAR4) (22), a finding further confirmed using pharmacological activation of GPR120 (25). The activation of the GPR120 receptor, which is mostly responsive to polyunsaturated fatty acids, has been reported to mediate potent anti-inflammatory and insulin sensitizing effects, and to protect against obesity and associated metabolic diseases (28). In our prior work (22), we also showed that activation of GPR120 in BAT and WAT promotes adaptive thermogenesis through the induction of FGF21 expression. Here, we show that, immediately after birth, an astonishingly high level of GPR120 expression is seen in BAT. Indeed, the expression levels of GPR120 in neonatal BAT are much higher than in any other mouse tissue at any other developmental stage. Based on these findings, we further analyzed the role of GPR120 in neonatal BAT adaptations.

81

82

MATERIALS AND METHODS

84 *Animals.* All animal experiments and selections of group sizes were performed in
85 accordance with European Community Council Directive 86/609/EEC and approved by
86 the Institutional Animal Care and Use Committee at the University of Barcelona. Swiss
87 mice (Envigo) and C57/BL6 GPR120-heterozygous mice (Ffar4tm1(KOMP)Vlclg;
88 MMRRC) were used. C57/BL6 GPR120-heterozygous mice were mated and
89 experiments were performed on the obtained GPR120^{-/-}, GPR120^{+/-}, and GPR120^{+/+}
90 littermates. For studies in fetuses, Cesarean sections were performed on day 19 of
91 gestation (E19). Neonates were studied at birth (0 hour, when all pups had been born
92 but had not yet started suckling), at 6 (P0.25), 12 (P0.5) and 24 (P1) hours after birth.
93 For ontogeny expression studies, Swiss mice were sampled at 7 (P7), 14 (P14), 21
94 (P21), and 70 (adult) days after birth. For studies on the effects of postnatal starvation
95 and environmental temperature, Swiss pups were separated from mothers prior to
96 initiation of suckling and placed in a humidified thermostatically controlled chamber at
97 21°C or 37°C for 8 hours. BAT temperature was non-invasively estimated by measuring
98 the iBAT skin-surface temperature using a high-sensitivity infrared thermography
99 camera (FLIR T33) as previously reported (22). Mice were killed by decapitation and
100 the liver, interscapular BAT, duodenum, jejunum, ileum, and colon were dissected.
101 Blood was collected, glucose levels were determined from a portion of the blood
102 sample using an Accutrend (Roche), and the remaining blood was centrifuged to obtain
103 plasma.

104 *Transmission electron microscopy.* BAT samples were fixed with 2.5%
105 glutaraldehyde and 2% paraformaldehyde in 0.1 M phosphate buffer (pH 7.4) and
106 post-fixed with 1% osmium tetroxide and 0.8% FeCNK in phosphate buffer. After
107 dehydration in a graded acetone series, tissue samples were embedded in Spurr resin.
108 Ultrathin sections were stained with uranyl acetate and lead citrate and examined with
109 a Jeol 1010 transmission electron microscope (Izasa Scientific, Barcelona, Spain), as
110 described previously (3).

111 *Glucose and palmitate oxidation.* Samples of interscapular BAT from 1-day-old (P1)
112 wild-type and GPR120^{-/-} pups were dissected. Pieces of BAT (~ 3 mg) were placed in
113 DMEM (Gibco) for 1 hour. Thereafter, the samples were incubated for 3 hours with
114 ¹⁴C-glucose (1 μCi/mL) (Perkin Elmer, NEC043X050UC) or ¹⁴C-palmitate (0.4 μCi/mL)
115 (NEC534050UC), the media were acidified, and the ¹⁴CO₂ released from incubated
116 explants was trapped into Whatman paper for 45 min. The impregnated Whatman
117 sheets were placed in Ecoscint H (National Diagnostics) and the dpm were quantified
118 using a Liquid Scintillation Analyzer (TRI-CARB 2100 TR, Packard Bioscience Company).

119 *RNA extraction and quantitative PCR with reverse transcription* RNA was extracted
120 from the tissue samples with a NucleoSpin® RNA kit (Macherey-Nagel, Düren,
121 Germany). Reverse transcription was performed using random hexamer primers
122 (Applied Biosystems, Foster City, CA, USA) and 0.5 μg RNA in a total reaction volume of
123 20 μl. For PCR, TaqMan Gene Expression Assay probes were used, with reaction
124 mixtures containing 1 μl cDNA, 10 μl TaqMan Universal PCR Master Mix (Applied

125 Biosystems), 250 nM probes, and 900 nM of primers from the Assays-on-Demand Gene
126 Expression Assay Mix (Applied Biosystems). The TaqMan probes used were : GPR120
127 (Ffar4), Mm00725193_m1; UCP1, Mm00494069_m1; Fgf21, Mm00840165_g1; Lpl,
128 Mm00434764_m1; Plin1, Mm00558672_m1; PPARalpha, Mm00440939_m1; Acox1,
129 Mm00443579_m1; Cpt1a, Mm01231183_m1; Ehhadh, Mm00619688_m1; 18S rRNA,
130 Hs99999901_s1. The 18S rRNA was measured as a housekeeping reference gene. The
131 mRNA level of each gene of interest in each sample was normalized to that of the
132 reference control using the comparative ($2^{-\Delta CT}$) method. A transcript was considered
133 to be non-detectable when $CT \geq 40$.

134 *Western blot and ELISA.* Western blot analysis of tissue extracts was performed
135 following standard procedures, using primary anti-UCP1 (1:1000 Abcam, Cambridge,
136 UK), and anti-GPR120 (1:150 sc-390752, Santa Cruz, USA). Loading controls were
137 established using antibodies against α -tubulin (T9026, Sigma-Aldrich) or GAPDH
138 (G9545, Sigma-Aldrich). Immunoreactive proteins were detected using an ECL
139 (enhanced chemiluminescence) system (GE Healthcare). Signal intensities were
140 quantified by scanning densitometry (Multi Gauge V3.0, Fujifilm). Plasma FGF21 levels
141 were quantified with ELISA (RD291108200R, Biovendor).

142 *Statistics.* Results are expressed as mean \pm SEM. Statistical analyses were
143 performed using GraphPad Prism 6 (La Jolla, CA, USA). The statistical significances of
144 differences were assessed using unpaired Student's t-tests, one-way ANOVA with
145 Tukey's multiple comparison tests, or two-way ANOVA with Bonferroni post-testing, as
146 appropriate.

147

148 **RESULTS AND DISCUSSION**

149 *High levels of Gpr120 expression in neonatal BAT.* The developmental regulation of
150 GPR120 mRNA expression in mouse BAT is shown in Figure 1a, where it is compared
151 with that in another tissue known to express the *Gpr120* gene (intestine sections) and
152 a tissue known to minimally express *Gpr120* (liver) (11,15,20). In adults, the expression
153 of the GPR120 transcript was significantly higher in BAT than in the other *Gpr120*-
154 expressing tissue (intestine), which is consistent with the previous data (22, 23).
155 GPR120 mRNA expression was low in fetal BAT as well as pups just born which did not
156 initiated suckling yet (P0); by just 6 hours post-partum, however, the GPR120 mRNA
157 level had increased so dramatically that it was much higher than those in adult BAT.
158 This high-level expression of the GPR120 mRNA in BAT was maintained during the first
159 days of life and declined progressively thereafter to reach adult levels. In the other
160 GPR120-expressing sites GPR120 transcript expression was higher in adults than in
161 neonates, and GPR120 mRNA levels tended to increase progressively throughout
162 development. The colon was unique in showing an early postnatal induction of *Gpr120*
163 gene expression, but the extent of this induction was much lower than that in BAT.
164 Assessment of GPR120 protein levels confirmed these trends and indicated that the
165 highest abundance of GPR120 was observed in neonatal BAT (Figure 1b).

166 *Post-natal thermal stress induces Gpr120 expression in BAT.* Given that GPR120 is a
167 lipid sensor, we tested whether the early postnatal induction of its mRNA in BAT could
168 be associated with the initiation of suckling or other events associated with birth, such
169 as thermal stress. For this purpose, mouse pups were studied under four different
170 conditions: just after birth but before suckling was initiated (0 hour) vs. 8 hours after
171 birth, having been maintained with the mother and confirmed to have suckled; or
172 having been separated from the mother before initiation of suckling and maintained
173 under non-feeding conditions at an environmental temperature of 21°C or 37°C. Our
174 results confirmed that GPR120 mRNA expression was induced in BAT at 8 hours after
175 delivery under feeding conditions and that this behavior was shared by BAT
176 thermogenesis-related genes, such as *Ucp1* and *Fgf21* (Figure 2). GPR120 transcript
177 expression was also induced in non-fed pups that were maintained at 21°C, whereas it
178 was totally blunted in non-fed pups maintained at 37°C (the same temperature as in
179 the intrauterine environment). Again, the behavior of *Gpr120* gene expression under
180 these conditions was similar to that of the thermogenesis-related genes, *Ucp1* and
181 *Fgf21*. In contrast, another gene unrelated to specific thermogenic activation but to
182 overall adipogenesis such as *PPARG* did not show a pattern of cold-induced expression
183 in the early neonatal period. Together, our results revealed that, similar to *Ucp1* and
184 *Fgf21*, the neonatal induction of *Gpr120* gene expression in BAT is mostly elicited by
185 postnatal thermogenic stress rather than by the initiation of feeding.

186 *Intolerance to post-natal cold in GPR120-null neonates.* Our observation that the
187 GPR120-coding gene is intensely regulated in neonatal BAT suggested that GPR120
188 could play a role in neonatal thermogenic adaptations. To analyze this possibility, we
189 studied GPR120^{-/-} (GPR120-KO) mouse neonates. Male and female C57/BL6 *Gpr120*
190 (*Ffar4*) ^{+/-} mice were mated, and females were maintained at a housing temperature
191 of 21°C during pregnancy and after delivery. At this temperature, the mortality of
192 GPR120^{-/-} pups at 1 day after birth was high (27.3%), while that of GPR120^{+/-} pups
193 was lower but still notable (16%) (Figure 3a). Increasing the environmental
194 temperature at delivery by 4°C (to 25°C) suppressed the mortality of GPR120^{-/-} pups.
195 These findings indicate that GPR120 plays a key role in the thermogenic adaptations
196 that occur during the neonatal period. For further studies, wild-type and GPR120^{-/-}
197 littermates were maintained at an environmental temperature of 25°C.

198 *Impaired thermogenic activity of BAT in GPR120-null pups.* Wild-type mice and
199 GPR120^{-/-} littermates were studied at E19, P0, P0.25, P0.5, P1 and P21. No significant
200 difference was observed in total body weight, BAT weight, or liver weight in GPR120^{-/-}
201 pups compared with wild-type neonates. Blood glucose levels did not show any major
202 between-genotype difference, although P1 GPR120^{-/-} pups showed decreased blood
203 glucose levels relative to wild-type littermates (Table 1). In wild-type littermates of
204 GPR120^{-/-} mice (C57/BL6 strain), we observed a strong postnatal induction of GPR120
205 mRNA similarly to what we observed in Swiss mice, although of lesser magnitude
206 (Figure 3b). Heat production by BAT was determined using infrared thermography at
207 the interscapular site of mouse pups, where the most prominent BAT depot is present.
208 Our data indicated that significantly less heat was produced by BAT in P1 GPR120^{-/-}

209 pups compared with wild-type neonates (Figure 3c). However, electron microscopy of
210 the cellular morphology of BAT samples did not reveal any massive alteration and only
211 a minor, non-significant, tendency to reduced lipid droplet size, due to *Gpr120* gene
212 loss-of-function (Fig. 3d).

213 The postnatal induction of *Ucp1* gene expression was significantly reduced in BAT
214 from GPR120^{-/-} mice at P0.25 and P0.5 and UCP1 mRNA levels remained lower at
215 postnatal day 21 (Figure 4a). UCP1 protein levels were also significantly lower in one
216 day-old GPR120^{-/-} pups relative to wild-type pups (Fig 4a). In fact, the GPR120^{-/-}
217 genotype was associated with a statistically significant reduction of UCP1 mRNA
218 ($P \leq 0.05$) and UCP1 protein ($P \leq 0.05$) levels when all of the studied neonates were
219 analyzed as a whole, according to two-way ANOVA factor analysis. UCP1 protein levels
220 and unmasking of the UCP1-mediated protein conductance are considered to be
221 essential for neonatal BAT thermogenesis (4, 21) and the altered levels of UCP1 found
222 in GPR120^{-/-} pups are consistent with reduced heat production in BAT.

223 Our analysis of the oxidative activity of BAT explants from P1 pups revealed that
224 lack of GPR120 did not alter the glucose oxidation rate, but was associated with a
225 dramatic reduction of fatty acid oxidation activity (Figure 4b). The expression of
226 transcript encoded by genes involved in lipid catabolism indicated a trend to be
227 reduced in BAT from GPR120^{-/-} pups, which was statistically significant for *Lpl* and
228 *Cpt1a* in neonates and for *Aox1* and *PPAR α* in fetuses at term (Figure 4c). Moreover,
229 the GPR120^{-/-} genotype was associated with a statistically significant reduction of
230 PLIN1 transcript ($P \leq 0.05$) when pups at the two distinct stages of development were
231 analyzed as a whole, according to two-way ANOVA factor analysis. Such trend was
232 maintained in mice studied at the age of weaning (P21) but only PLIN1 mRNA levels
233 were significantly decreased in GPR120^{-/-} mice relative to wild-type controls at that
234 age (Fig 4c). Collectively, these data indicate the GPR120 is necessary for the adaptive
235 thermogenic activation of neonatal BAT, but that it does not determine the cell
236 differentiation or acquisition of gross BAT structure during neonatal development. The
237 impairment in fatty acid oxidation pathways in BAT due to the lack of functional
238 GPR120, occurring in concert with impaired BAT thermogenesis, is consistent with the
239 preferential usage of fatty acids as metabolic sources for sustaining heat production in
240 BAT (2). The impact of GPR120 loss-of-function in neonatal mice (compromised
241 survival associated with impaired BAT function, and its rescue by high environment
242 temperature) is reminiscent of similar observations in mice with targeted mutations of
243 genes encoding key regulators of BAT development and function such as PACAP, a
244 controller of norepinephrine release to BAT (9), PREF1 and DIO3 (5), and UCP1 itself
245 (4). This highlights the importance of appropriate BAT function for postnatal
246 thermoregulation and the key role of GPR120 in this process.

247 *GPR120 is required for the induction of FGF21 expression in BAT and FGF21 rise in*
248 *blood from neonates.* Previous reports showed that FGF21 plasma levels were
249 increased during the first days of life in mice (12), and we previously found that
250 GPR120^{-/-} adult mice show reduced FGF21 circulating levels upon cold exposure (22).

251 The induction of FGF21 after birth is considered a neonatal-period adaptation that
252 contributes to BAT thermogenesis (12). We herein found that pups deficient for
253 GPR120 show impaired postnatal induction of plasma FGF21 levels at P0.5 and P1 and
254 decreased levels of FGF21 were also present at P21 (Figure 5a). The FGF21 present in
255 neonatal blood is considered to have a mainly hepatic origin (12), although adult BAT is
256 known to express and release significant amounts of FGF21 when thermogenesis is
257 activated (13). We found that FGF21 mRNA expression is markedly induced in BAT in
258 the first hours of life, and that such induction is strongly impaired in GPR120^{-/-} pups.
259 Also, the postnatal increase in FGF21 mRNA expression in the liver was not affected by
260 GPR120 gene loss-of-function (Figure 5b). Thus, we conclude that the effects of
261 GPR120 on neonatal adaptation involve alterations of the FGF21 system in BAT, which
262 may have consequences in systemic levels of FGF21. Considering previous data on the
263 effects of FGF21 in BAT (12, 26), impaired signaling of FGF21 may be involved in the
264 reduction in *Ucp1* gene expression and fatty acid oxidation in GPR120-null neonates.

265 In summary, we herein show that the GPR120-dependent pathway is essential for
266 inducing adaptive neonatal BAT thermogenesis and the control of the FGF21 system.
267 GPR120 (FFAR4) is considered a receptor for long chain fatty acids, preferentially of the
268 n-3 PUFA type (18). N-3 PUFAs have been reported to induce brown fat activity in adult
269 mice and in brown adipocytes in culture through interaction with GPR120 (16, 22).
270 Initiation of lactation is associated with a massive and sudden intake of the lipids
271 present in milk, including n-3 PUFAs (7), in the neonates, in contrast with the
272 predominant glucose-based metabolic supply in the fetal period. Although we found
273 that GPR120 expression itself is mostly regulated by cold stress rather than milk intake,
274 our findings are consistent with the notion that fatty acids from milk may be essential
275 regulators of neonatal thermogenic activation through the activation of the highly
276 expressed GPR120 in BAT.

277 The current findings of a key role of GPR120 in energy metabolism in neonates may
278 have relevant implications for neonatal and adult metabolic health. Although gene
279 expression of GPR120 in human neonatal tissues is unknown, recent findings
280 evidenced a postnatal surge in the levels of FGF21 (a main target of GPR120-
281 dependent regulation according to our data above) in human neonates (24),
282 analogously to rodents. However, the intensity of postnatal thermal stress in humans
283 is likely to be lower than in rodents and, therefore, induction of GPR120 might be
284 milder in human neonates. Moreover, a deleterious non-synonymous mutation that
285 inhibits GPR120 signaling activity has been identified in human individuals, which
286 increase the risk of obesity (14). However, in GPR120-deficient mice, obesity develops
287 only after a high-fat diet (14). Thus, a similar quantitative role of GPR120 in energy balance
288 among different species can not be assumed unequivocally. In any case, the strong impact of
289 appropriate GPR120 signaling in the neonatal period metabolism found in mouse
290 models may be of utmost importance not only in relation to perinatal health but also
291 in relation to the adult consequences that metabolic alterations in early development
292 may have.

293

294 **AUTHOR CONTRIBUTIONS**

295 TQL, SMR, and LC performed the animal experiments and monitoring of the pup
296 deliveries. RI, AGN, and TQL performed the cesarean sections for fasting tests,
297 differential temperature exposure experiments and substrates' oxidation assays. TQL,
298 AGN and LC performed that quantitative analysis of transcripts and proteins. MG, FV,
299 and TQL performed the data analysis and statistics; also cooperated in the writing of
300 the article. All authors revised and accepted the manuscript details.

301 **DISCLAIMERS**

302 The authors declare that no conflicts of interest exist.

303 **ACKNOWLEDGMENTS**

304 We thank M. Morales and A. Perú for their help with the sample management.

305 **GRANTS**

306 This research was supported by grants from Ministerio de Economía y Competitividad
307 (SAF2017-85722) and Fondo de Investigaciones Sanitarias, Instituto de Salud Carlos III
308 (PI17/00420), co-financed by the European Regional Development Fund (ERDF). TQL
309 thanks CONACyT (Consejo Nacional de Ciencia y Tecnología, México) for PhD
310 scholarship.

311

312 **REFERENCES**

313 **1. Asakura H.** Fetal and neonatal thermoregulation. *Journal of Nippon Medical School* 71: 360-
314 370, 2004.

315 **2. Bartelt A, Bruns OT, Reimer R, Hohenberg H, Ittrich H, Peldschus K, Kaul MG, Tromsdorf**
316 **UI, Weller H, Waurisch C, Eychmüller A, Gordts PL, Rinninger F, Bruegelmann K, Freund B,**
317 **Nielsen P, Merkel M, Heeren J.** Brown adipose tissue activity controls triglyceride clearance.
318 *Nat Med.* 17:200-205, 2011.

319 **3.Cairó M, Villarroya J, Cereijo R, Campderrós L, Giralte M, Villarroya F.** Thermogenic
320 activation represses autophagy in brown adipose tissue. *Int J Obes (Lond)* 40: 1591-1599,
321 2016.

322 **4.Cannon B, Nedergaard J.** Brown adipose tissue: function and physiological significance.
323 *Physiol Rev* 84: 277-359, 2004

324 **5. Charalambous M, Ferron SR, da Rocha ST, Murray AJ, Rowland T, Ito M, Schuster-Gossler**
325 **K, Hernandez A, Ferguson-Smith AC.** Imprinted gene dosage is critical for the transition to
326 independent life. *Cell Metab.* 15:209-221, 2012.

327 **6. Fisher FM, Kleiner S, Douris N, Fox EC, Mepani RJ, Verdeguer F, Wu J, Kharitonov A,**
328 **Flier JS, Maratos-Flier E, Spiegelman BM.** FGF21 regulates PGC-1 α and browning of white
329 adipose tissues in adaptive thermogenesis. *Gene Dev* 26:271-281, 2012.

- 330 **7. Gavaldà-Navarro A, Hondares E, Giralt M, Mampel T, Iglesias R, Villarroya F.** Fibroblast
331 growth factor 21 in breast milk controls neonatal intestine function. *Sci Rep.* 5:13717, 2015.
- 332 **8. Giralt M, Martin I, Iglesias R, Viñas O, Villarroya F, Mampel T.** Ontogeny and perinatal
333 modulation of gene expression in rat brown adipose tissue. Unaltered iodothyronine 5'-
334 deiodinase activity is necessary for the response to environmental temperature at birth. *Eur J*
335 *Biochem* 193: 297-302, 1990.
- 336 **9. Gray SL, Yamaguchi N, Vencová P, Sherwood NM.** Temperature-sensitive phenotype in
337 mice lacking pituitary adenylate cyclase-activating polypeptide. *Endocrinology* 143:3946-54,
338 2002.
- 339 **10. Gunn TR, Gluckman PD.** Perinatal thermogenesis. *Early Hum Dev.* 42:169-183, 1995
- 340 **11. Hirasawa A, Tsumaya K, Awaji T, Katsuma S, Adachi T, Yamada M, Sugimoto Y, Miyazaki**
341 **S, Tsujimoto G.** Free fatty acids regulate gut incretin glucagon-like peptide-1 secretion through
342 GPR120. *Nat Med* 11:90-94, 2005.
- 343 **12. Hondares E, Rosell M, Gonzalez FJ, Giralt M, Iglesias R, Villarroya F.** Hepatic FGF21
344 expression is induced at birth via PPARalpha in response to milk intake and contributes to
345 thermogenic activation of neonatal brown fat. *Cell Metab* 11: 206-212, 2010.
- 346 **13. Hondares E, Iglesias R, Giralt A, Gonzalez FJ, Giralt M, Mampel T, Villarroya F.**
347 Thermogenic activation induces FGF21 expression and release in brown adipose tissue. *J Biol*
348 *Chem.* 286:12983-12990, 2011.
- 349 **14. Ichimura A, Hirasawa A, Poulain-Godefroy O, Bonnefond A, Hara T, Yengo L, Kimura I,**
350 **Leloire A, Liu N, Iida K, Choquet H, Besnard P, Lecoœur C, Vivequin S, Ayukawa K, Takeuchi M,**
351 **Ozawa K, Tauber M, Maffei C, Morandi A, Buzzetti R, Elliott P, Pouta A, Jarvelin MR, Körner**
352 **A, Kiess W, Pigeyre M, Caiazzo R, Van Hul W, Van Gaal L, Horber F, Balkau B, Lévy-Marchal C,**
353 **Rouskas K, Kouvatsi A, Hebebrand J, Hinney A, Scherag A, Pattou F, Meyre D, Koshimizu TA,**
354 **Wolowczuk I, Tsujimoto G, Froguel P.** Dysfunction of lipid sensor GPR120 leads to obesity in
355 both mouse and human. *Nature.* 483:350-354, 2012
- 356 **15. Iwasaki K, Harada N, Sasaki K, Yamane S, Iida K, Suzuki K, Hamasaki A, Nasteska D,**
357 **Shibue K, Joo E, Harada T, Hashimoto T, Asakawa Y, Hirasawa A, Inagaki N.** Free fatty acid
358 receptor GPR120 is highly expressed in enteroendocrine K cells of the upper small intestine
359 and has a critical role in GIP secretion after fat ingestion. *Endocrinology* 156:837-46, 2015.
- 360 **16. Kim J, Okla M, Erickson A, Carr T, Natarajan SK, Chung S.** Eicosapentaenoic Acid
361 Potentiates Brown Thermogenesis through FFAR4-dependent Up-regulation of miR-30b and
362 miR-378. *J Biol Chem.* 291:20551-20562, 2016.
- 363 **17. Lidell ME.** Brown Adipose Tissue in Human Infants. *Handb Exp Pharmacol.* 251:107-112,
364 2019.
- 365 **18. Milligan G, Shimpukade B, Ulven T, Hudson BD.** Complex Pharmacology of Free Fatty Acid
366 Receptors. *Chem Rev.* 117 :67-110, 2017
- 367 **19. Nedergaard J, Connolly E, Cannon B.** Brown adipose tissue in the mammalian neonate . In:
368 *Brown Adipose Tissue*, edited by Trayhurn P, Nicholls DG. Edward Arnold, London, 1986, p152-
369 213.

- 370 **20. Paulsen S J, Larsen L K, Hansen G, Chelur S, Larsen P J, Vrang N.** Expression of the Fatty
371 Acid Receptor GPR120 in the Gut of Diet-Induced-Obese Rats and Its Role in GLP-1 Secretion.
372 *PLoS One* 9: e88227, 2014.
- 373 **21. Porras A, Peñas M, Fernández M, Benito M .**Development of the uncoupling protein in the
374 rat brown-adipose tissue during the perinatal period. Its relationship with the mitochondrial
375 GDP-binding and GDP-sensitive ion permeabilities and respiration. *Eur J Biochem.* 187:671-675,
376 1990.
- 377 **22. Quesada-López T, Cereijo R, Turatsinze JV, Planavila A, Cairó M, Gavaldà-Navarro A,**
378 **Peyrou M, Moure R, Iglesias R, Giralt M, Eizirik DL, Villarroya F.** The lipid sensor GPR120
379 promotes brown fat activation and FGF21 release from adipocytes. *Nat Commun.* 7:13479,
380 2016.
- 381 **23. Rosell M, Kaforou M, Frontini A, Okolo A, Chan YW, Nikolopoulou E, Millership S, Fenech**
382 **ME, MacIntyre D, Turner JO, Moore JD, Blackburn E, Gullick WJ, Cinti S, Montana G, Parker**
383 **MG, Christian M.** Brown and white adipose tissues: intrinsic differences in gene expression and
384 response to cold exposure in mice. *Am J Physiol Endocrinol Metab* 306:E945-964, 2014.
- 385 **24. Sánchez-Infantes D, Gallego-Escuredo JM, Díaz M, Aragonés G, Sebastiani G, López-**
386 **Bermejo A, de Zegher F, Domingo P, Villarroya F, Ibáñez L.** Circulating FGF19 and FGF21 surge
387 in early infancy from infra- to supra-adult concentrations. *Int J Obes (Lond).* 39:742-746, 2015.
- 388 **25. Schilperoort M, van Dam AD, Hoeke G, Shabalina IG, Okolo A, Hanyaloglu AC, Dib LH, Mol**
389 **IM, Caengprasath N, Chan YW, Damak S, Miller AR, Coskun T, Shimpukade B, Ulven T,**
390 **Kooijman S, Rensen PC, Christian M.** The GPR120 agonist TUG-891 promotes metabolic health
391 by stimulating mitochondrial respiration in brown fat. *EMBO Mol Med.* 10: e8047, 2018
- 392 **26. Schlein C, Talukdar S, Heine M, Fischer AW, Krott LM, Nilsson SK, Brenner MB, Heeren J,**
393 **Scheja L.** FGF21 Lowers Plasma Triglycerides by Accelerating Lipoprotein Catabolism in White
394 and Brown Adipose Tissues. *Cell Metab.* 23:441-453, 2016.
- 395 **27. Symonds ME, Pope M, Budge H.** The Ontogeny of Brown Adipose Tissue. *Annu Rev Nutr.*
396 35:295-320, 2015.
- 397 **28 .Talukdar S, Olefsky JM, Osborn O.** Targeting GPR120 and other fatty acid-sensing GPCRs
398 ameliorates insulin resistance and inflammatory diseases. *Trends Pharmacol Sci.* 32:543-550,
399 2011.
- 400
- 401

402 **Figure legends**

403 **Figure 1. Developmental regulation of GPR120 gene expression.** (a) Relative
404 transcript levels of GPR120 (FFAR4) in tissues from Swiss mice obtained at the indicated
405 developmental time points. E19, fetuses, embryonic day 19; A, adults, 70 days old. (b)
406 Representative immunoblot of GPR120 (FFAR4) protein levels in BAT (left), ileum and
407 colon (right). Images correspond to equally loaded lanes with identical incubation
408 conditions and exposure time. Bars are means + sem of 4-10 pups from at least 3
409 independent litters. One-way ANOVA was performed and the statistically significant
410 differences are shown as *P<0.05, **P<0.01, and ***P<0.001 compared to E19.

411
412 **Figure 2. Effects of post-natal fasting and cold stress on GPR120 gene expression in**
413 **BAT.** Relative transcript levels of GPR120, Fgf21, UCP1 and PPAR γ in neonates at birth
414 (0h, before initiation of suckling) and 8-hour-old pups that had been allowed to suckle
415 (Fed) or not allowed to suckle (Fasted) and maintained at environmental temperatures
416 of 21°C or 37°C. Bars are means \pm sem of 4-10 pups from at least 3 independent litters.
417 One-way ANOVA was performed and the statistically significant differences are shown
418 as *P<0.05, **P<0.01, and ***P<0.001 compared to E19.

419
420 **Figure 3. Effects of GPR120 gene loss-of-function on BAT in the perinatal period.** (a)
421 Aggregate survival rates of GPR120 $^{-/-}$, GPR120 $^{+/-}$ and wild-type neonates during the
422 first hours of life. (b) Relative transcript levels of GPR120 in tissues from C57/BL6
423 GPR120 $^{+/+}$ neonatal mice at the indicated developmental time points. (c)
424 Representative infrared thermography images (left) and surface temperature
425 quantifications from interscapular BAT areas (right) of 1-day-old GPR120 $^{-/-}$ pups and
426 wild-type littermates. (d) Representative transmission electron microscopic images
427 (scale bar: 10 μ m) of interscapular BAT (up) and lipid droplet area in BAT (down). Data
428 are presented as means \pm sem from 5-7 individual samples from at least 4 different
429 litters. Statistically significant differences are shown as *P<0.05 (one-way ANOVA) for
430 comparison with E19 and +P<0.05 (two-tailed unpaired Student's t-test) for
431 comparison between GPR120 $^{-/-}$ and wild-type littermates.

432
433 **Figure 4. Effects of GPR120 gene loss-of-function on UCP1 expression, glucose**
434 **oxidation and fatty acid oxidation in BAT.** (a) Relative transcript levels of UCP1 (left)
435 and UCP1 protein levels (right) in BAT from GPR120 $^{-/-}$ pups and wild-type littermates
436 at the indicated postnatal times. Representative immunoblot of UCP1 protein is shown
437 (bottom of right panel). α -tubulin (ATUB), loading control. (b) Relative levels of 14 C $_2$
438 production from 14 C-Glucose and 14 C-Palmitate in BAT explants from 1-day-old pups
439 incubated for 3 hours. (c) Relative transcript levels of the indicated gene in BAT from
440 GPR120 $^{-/-}$ fetuses, 6h-old neonates, and 21 day-old (weaning) mice, and wild-type
441 littermates. Data are presented as means \pm sem of 5-9 individuals from at least 5
442 different litters. Two-way ANOVA was performed and statistically significant
443 differences are shown as *P<0.05, **P<0.01, and ***P<0.001 compared with E19, and

444 + P<0.05 for comparison between GPR120^{-/-} pups and wild-type littermates at each
445 age.

446

447 **Figure 5. FGF21 gene expression in neonatal GPR120-null mice.** GPR120^{-/-} pups and
448 wild-type littermates were studied at the indicated ages. (a) Plasma levels of FGF21. (b)
449 Relative transcript levels of Fgf21 in BAT. (c) Relative transcript levels of Fgf21 in liver.
450 Data are presented as means \pm sem of 5-9 individuals belonging to at least 5 different
451 litters. Two-way ANOVA was performed and statistically significant differences are
452 shown as *P<0.05, **P<0.01, and ***P<0.001 compared with the corresponding
453 controls at E19; and as +P<0.05 and ++P<0.01 for comparison of GPR120^{-/-} relative to
454 wild-type pups at each age.

455

456

457

458

Figure 1

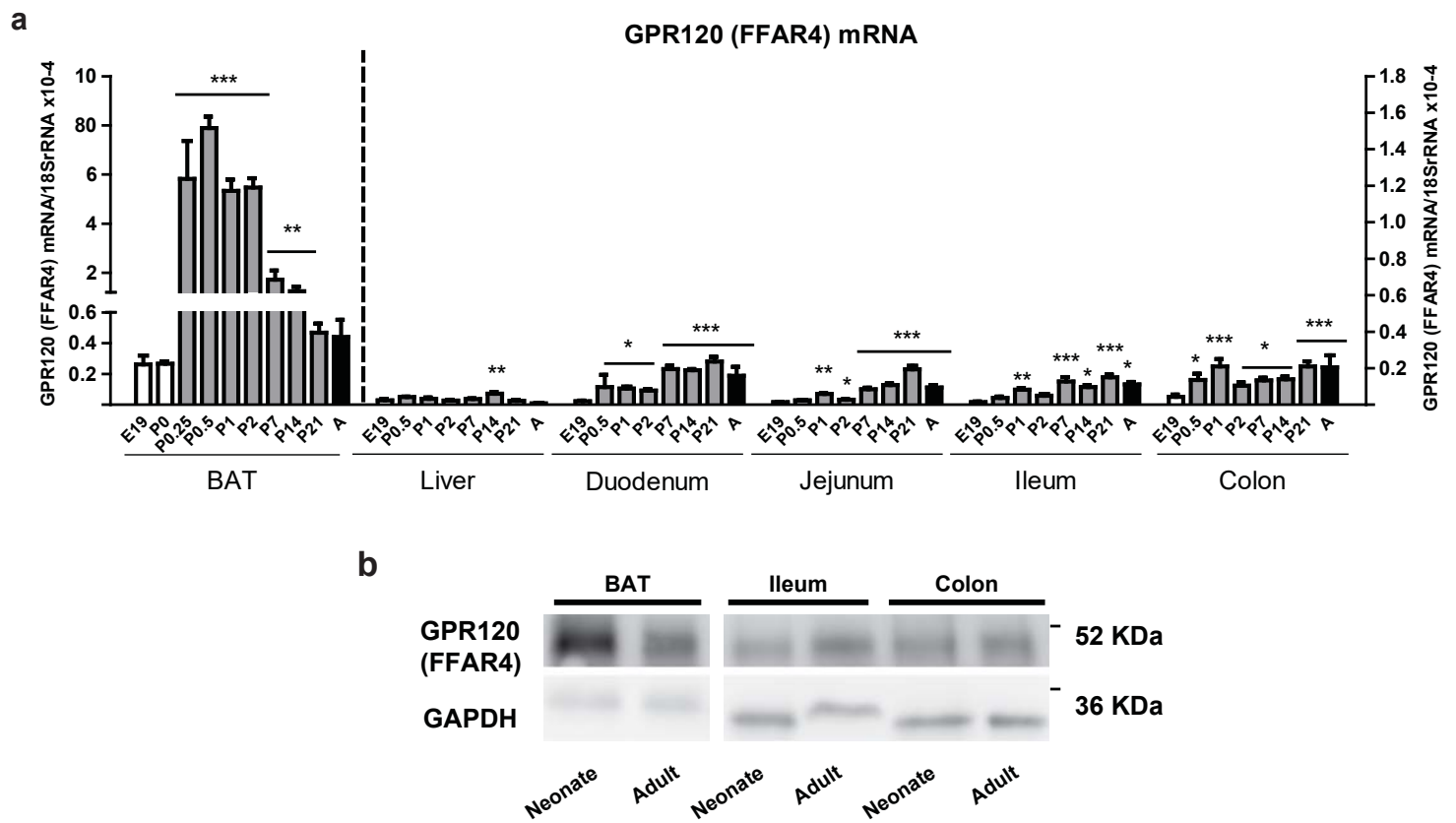


Figure 2

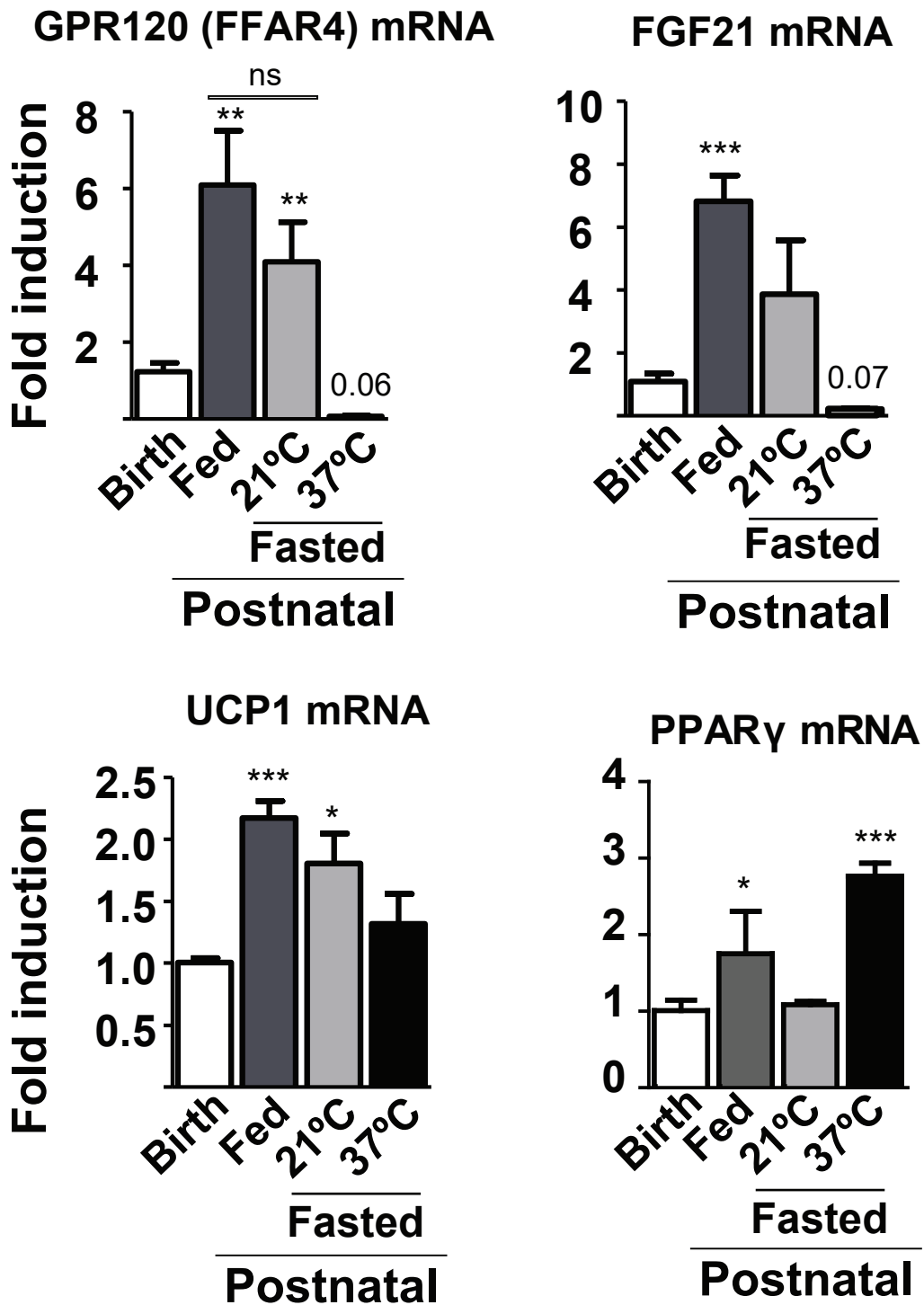


Figure 3

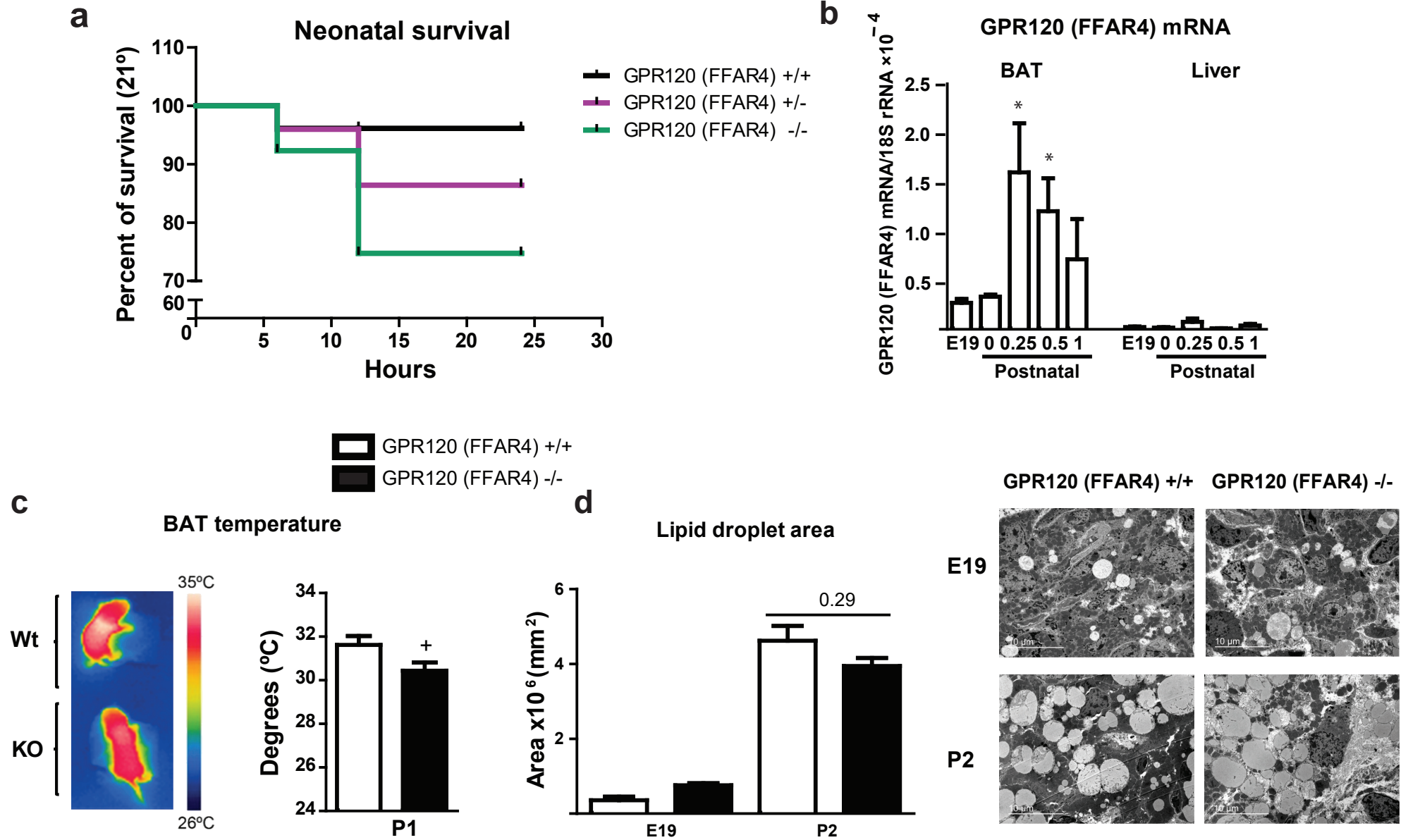
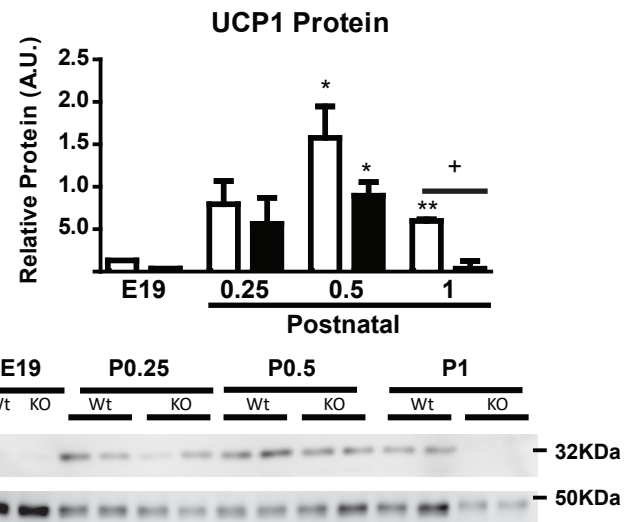
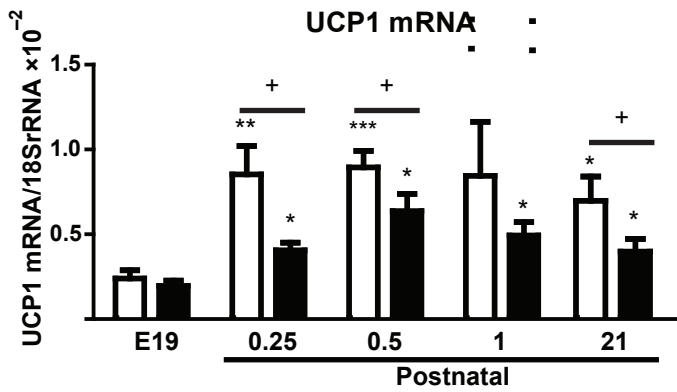


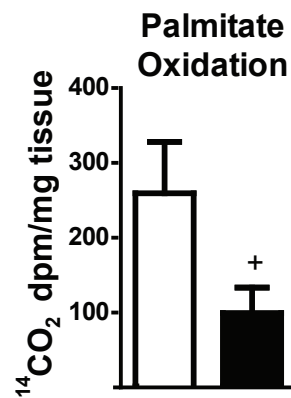
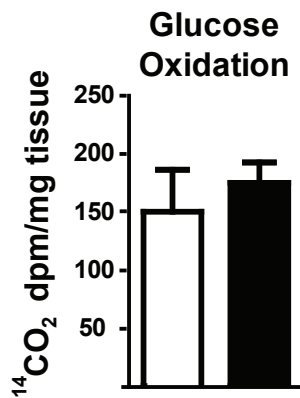
Figure 4

□ GPR120 (FFAR4) +/+
 ■ GPR120 (FFAR4) -/-

a



b



c

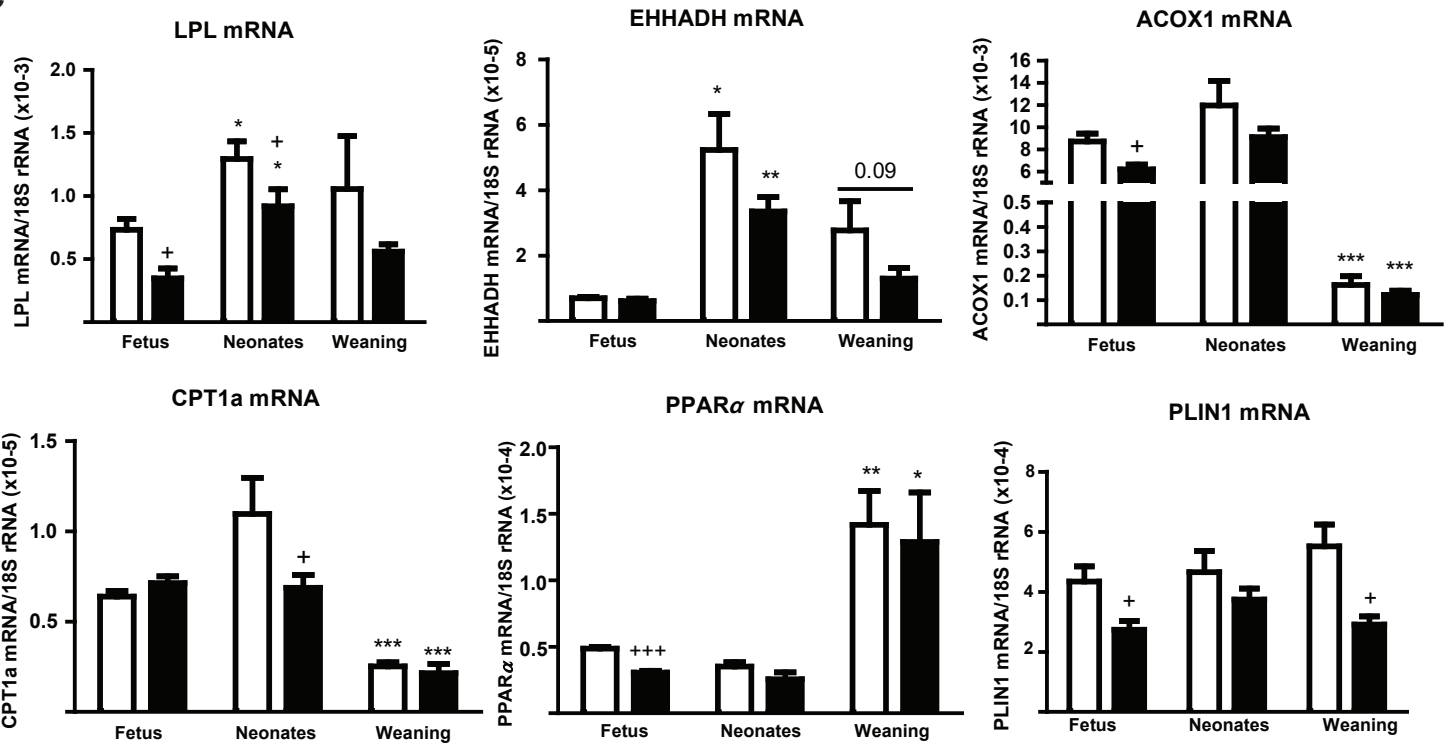
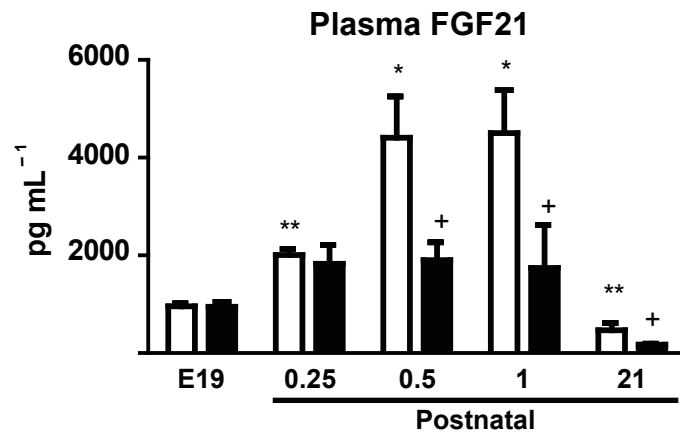


Figure 5

□ GPR120 (FFAR4) +/+
■ GPR120 (FFAR4) -/-

a



b

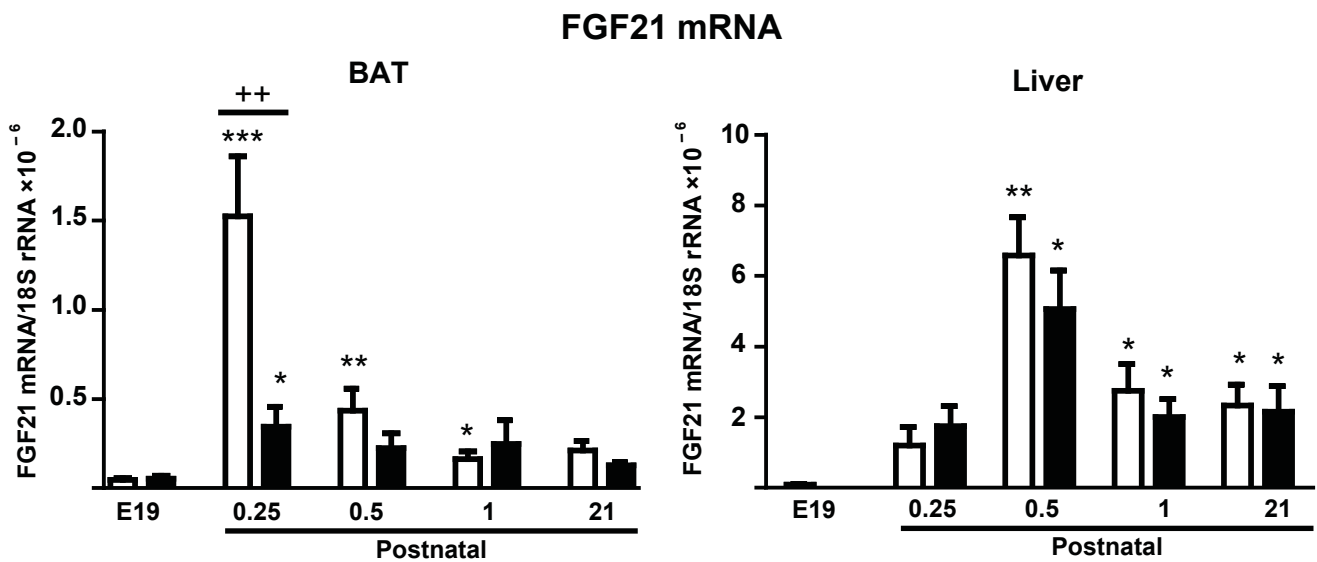


Table 1. Body weight, BAT and liver weights, and blood glucose											
	Fetus (E19)		6 h (P 0.25)		12 h (P 0.5)		24h (P 1)		P21		P value
	Wild-type	GPR120 (FFAR4) -/-	Wild-type	GPR120 (FFAR4) -/-	Wild-type	GPR120 (FFAR4) -/-	Wild-type	GPR120 (FFAR4) -/-	Wild-type	GPR120 (FFAR4) -/-	
Body Weight (BW) (g)	1.1 ± 0.05	1.0 ± 0.05	1.3 ± 0.03	1.3 ± 0.06	1.4 ± 0.05	1.3 ± 0.07	1.4 ± 0.07	1.4 ± 0.04	9.9 ± 0.2	9.8 ± 0.3	0,12
BAT Weight (mg/g BW)	9.0 ± 0.5	9.3 ± 1.2	7.2 ± 0.5	6.6 ± 0.6	7.2 ± 0.6	7.6 ± 0.7	6.3 ± 0.4	6.2 ± 0.3	4.9 ± 0.6	5.3 ± 0.3	0,70
Liver Weight (mg/g BW)	55.1 ± 1.9	46.0 ± 4.1	37.8 ± 1.3*	42.9 ± 1.5 +	37.0 ± 1.1	37.6 ± 1.6	33.8 ± 1.3	31.7 ± 2.4	43.7 ± 4.6	45.0 ± 2.4	0,41
Glucose (mg/dL)	52.8 ± 10.6	48.0 ± 5	60.0 ± 2.6	63.6 ± 10.5	63.7 ± 5.2	62.9 ± 4.9	81.0 ± 4.1	63.8 ± 4.9 +	154.8 ± 10.1	172.0 ± 15.5	0,93
Data are means ± SEM of 5 to 11 pups per group from at least 4 independent litters. Two-way ANOVA analysis was employed for determining genotype differences in expression (*P<0.05 for comparison between each age and its corresponding control; +P<0.05 for comparison between WT and GPR120-/- at a given age).											